JHWCR JOURNAL OF HEALTH, WELLNESS AND COMMUNITY RESEARCH 3007-0570

https://doi.org/10.61919/zhzayt81

Original Article

In Silico Analysis of Extremophilic Bacteria Isolated from Food-Service Environments in Lahore

Anam Amir[1], Ayesha Ahmed[1], Bisma Ali[1], Anam Amar[1], Haleema Sadia[1], Mamona Imran[1]

[1] Department of Life Sciences, University of Management and Technology, Lahore, Pakistan

***Corresponding author: Anam Amir. Email: anam.amir@umt.edu.pk**

"Cite this Article" Received: 11 March 2026; **Accepted**: 22 April 2026; **Published**: 03 May 2026

Author Contributions: AAm conceived and supervised the study. AAh, BA, AAr, HS, and MI performed sample collection, microbiological work, and in silico analyses. AAm and AAh drafted the manuscript. All authors reviewed and approved the final version. **Ethical Approval**: University of Management and Technology, Lahore, Pakistan. **Informed Consent**: Written informed consent was obtained from all participants; **Conflict of Interest**: The authors declare no conflict of interest. **Funding**: No external funding; **Data Availability**: Available from the corresponding author on reasonable request; **Acknowledgments**: N/A.

ABSTRACT

Background: Food-service surfaces in dense urban settings act as reservoirs for Enterobacteriaceae, and routine alkaline sanitation may select for pH-tolerant organisms. Enterobacter bugandensis has emerged as a multidrug-resistant pathogen, yet its recovery from food-contact surfaces in South Asian settings remains poorly characterised. Objective: To isolate alkali-tolerant bacteria from high-contact dining surfaces in Lahore, Pakistan, and computationally evaluate the haemolysin-coregulated protein (Hcp) of the Type VI secretion system and the heme transporter ChuA as candidate inhibitor targets. Methods: In this cross-sectional laboratory-based study, sterile swabs were collected from high-contact surfaces in thirty restaurants. Isolates were recovered on nutrient agar, screened across pH 7–10, and characterised by staining, biochemical profiling, and bidirectional 16S rRNA Sanger sequencing. Phylogeny was inferred in MEGA X. Hcp and ChuA were modelled by SWISS-MODEL and validated by Ramachandran and MolProbity analysis. Binding pockets were predicted by PrankWeb. Three matrix metalloprotease inhibitors were docked into Hcp and five heme analogues into ChuA using CB-Dock2 (AutoDock Vina), ranked by predicted binding energy. Results: A dominant alkali-tolerant Gram-negative bacillus grew sustainably at pH 10. Biochemical profile matched Enterobacter; 16S rRNA BLASTn returned closest identity to Enterobacter bugandensis (96.12%). The Hcp model achieved GMQE 0.92 with 98.39% favoured Ramachandran residues. Ilomastat returned the most favourable Hcp binding energy (–6.3 kcal/mol), engaging R26, D25, and Y99. Mn(III) and Ru(III) protoporphyrin IX both yielded –7.4 kcal/mol against ChuA, though template and ligand-identity limitations restrict interpretation. Conclusion: An alkali-tolerant Enterobacter closely related to E. bugandensis persisted on routinely cleaned dining surfaces, indicating that conventional sanitation may inadequately eliminate clinically relevant Enterobacteriaceae. Ilomastat emerged as a candidate Hcp inhibitor; ChuA findings require re-validation. Routine molecular surveillance of food-contact surfaces is warranted. Keywords: Enterobacter bugandensis; alkali tolerance; food-service hygiene; Type VI secretion system; ChuA; molecular docking; Ilomastat; protoporphyrin IX; antivirulence; Pakistan.

INTRODUCTION

Foodborne disease remains a substantial global public-health burden, and food-service environments are now recognized as critical control points along the farm-to-fork chain. In dense urban settings with rapidly expanding restaurant sectors, high-contact dining surfaces — including tables, cutlery, serving trays, and beverage equipment — function as reservoirs for microbial transfer between food handlers, utensils, and consumers (1). Surveillance studies across multiple regions have repeatedly recovered Escherichia coli, Staphylococcus aureus, Salmonella enterica, Listeria monocytogenes, and members of the Enterobacteriaceae from such surfaces, with contamination consistently linked to inadequate handwashing, poor sanitation discipline, and inconsistent maintenance of food-contact equipment (2,3).

Routine sanitation in food-service settings relies heavily on alkaline detergents and chlorine-based disinfectants. Although effective against most vegetative bacteria, repeated exposure to alkaline cleaning regimens exerts a selective pressure that favours organisms capable of surviving extreme pH conditions. Alkaliphilic and alkali-tolerant bacteria can grow at pH ≥ 9 and have been characterized in both natural and engineered environments (4). Their persistence on food-contact surfaces despite routine cleaning challenges the assumption that conventional sanitation guarantees microbiological safety, and creates a niche in which clinically significant alkali-tolerant pathogens may go undetected by standard hygiene monitoring (5).

Among the emerging Enterobacteriaceae of concern, Enterobacter bugandensis has rapidly gained recognition as a multidrug-resistant pathogen, first described in neonatal blood cultures from Tanzania and subsequently reported across diverse clinical and environmental settings (6). Reported associations include neonatal sepsis with mortality rates of 40–60%, ventilator-associated pneumonia, catheter-associated urinary tract infections, and bloodstream infections in immunocompromised adults (7). Genomic surveys consistently identify extended-spectrum β-lactamase determinants and carbapenemase-associated genes, while phenotypic studies highlight prolonged survival on dry surfaces, biofilm-forming capacity, and partial tolerance of common disinfectants (8). Despite these features, the recovery of E. bugandensis from food-service environments remains poorly documented, particularly in lower- and middle-income urban settings where dining out is a frequent dietary pattern.

Targeted disruption of bacterial virulence offers a complementary strategy to conventional antibiotic-based control. The Type VI secretion system (T6SS), built around the haemolysin-coregulated protein (Hcp) tube, mediates contact-dependent toxin delivery to competing microbes and host cells, while the outer-membrane heme transporter ChuA enables iron acquisition essential for colonization and persistence in mammalian hosts (9). Both proteins are amenable to in silico inhibitor screening: homology modelling, binding-site prediction, and molecular docking allow rapid evaluation of candidate inhibitors prior to wet-lab validation, an approach that has accelerated antivirulence discovery for several Gram-negative pathogens (10,11).

Despite the clinical importance of E. bugandensis and the public-health relevance of alkali-tolerant survivors on food-contact surfaces, integrated studies that link environmental isolation with structural-bioinformatics characterization of virulence proteins are lacking, particularly in South Asian urban settings. The present study addresses this gap by isolating alkali-tolerant bacteria from high-contact surfaces in restaurants across Lahore, identifying the predominant isolate using phenotypic, biochemical, and 16S rRNA-based approaches, and computationally evaluating Hcp and ChuA as candidate targets for inhibitor binding through homology modelling and molecular docking.

MATERIALS AND METHODS

This was a cross-sectional laboratory-based study conducted between [study period to be inserted by authors] in Lahore, Pakistan, combining environmental bacterial isolation with in silico characterization of two putative virulence proteins. Thirty restaurants representing a range of socioeconomic settings — from informal street-food outlets to upmarket cafes — were purposively selected to capture the diversity of food-service environments in the city. High-contact surfaces, comprising dining tables, serving trays, and cutlery, were sampled aseptically using sterile cotton swabs moistened with sterile physiological saline. A standardized zigzag swabbing motion was applied across a defined surface area, and swabs were transferred immediately into sterile labelled transport tubes. All samples reached the microbiology laboratory of the Department of Life Sciences, University of Management and Technology, within two to three hours of collection to preserve microbial viability.

Each swab was streaked onto nutrient agar (peptone 10 g/L, yeast extract 5 g/L, sodium chloride 10 g/L, agar 15 g/L; final pH 7.0 ± 0.2) prepared in distilled water and autoclaved at 121 °C for 15 minutes. Plates were incubated aerobically at 37 °C for 24 h, after which morphologically distinct colonies were sub-

cultured into nutrient broth and re-streaked sequentially until pure cultures were obtained, with purity confirmed by uniform colony morphology and Gram-stain consistency. Pure isolates were preserved at 4 ˚C for short-term working use and as 20% glycerol stocks at –80 ˚C for long-term storage.

Alkali tolerance of each pure isolate was screened by sub-culturing on nutrient agar adjusted with sterile 1 M NaOH to pH 7, 8, 9, and 10. The pH of each batch was verified after autoclaving using a calibrated bench-top pH meter. Growth was recorded after 24 h of incubation at 37 ˚C, and isolates showing visible growth at pH ≥ 9 were classified as alkali-tolerant and retained for further characterization. Phenotypic characterization included colony morphology assessment together with methylene blue staining, Gram staining, and Ziehl–Neelsen acid-fast staining performed according to standard protocols and examined under oil-immersion light microscopy at 1000× magnification. Biochemical identification followed conventional methods, including oxidase, catalase, urease, indole, citrate utilization, methyl red, Voges–Proskauer, motility, and carbohydrate fermentation tests, with results interpreted against published reference profiles for the Enterobacteriaceae.

Genomic DNA was extracted from overnight broth cultures using the Qiagen DNeasy Mini Kit (Qiagen, Hilden, Germany) following the manufacturer's protocol. The 16S rRNA gene was amplified by polymerase chain reaction (PCR) using universal bacterial primers 27F and 1492R, and amplicons were submitted for bidirectional Sanger sequencing to Apical Scientific Sdn. Bhd. (formerly First BASE Laboratories Sdn. Bhd., Selangor, Malaysia). Forward and reverse reads were assembled and manually edited using BioEdit, and the consensus sequence was queried against the NCBI nucleotide database using BLASTn to identify the closest matching taxa. Phylogenetic relationships were inferred in MEGA X using the Fast Minimum Evolution algorithm with a maximum sequence-difference threshold of 0.75.

For in silico characterization of virulence proteins, the amino-acid sequences of the haemolysin-coregulated protein (Hcp) of the T6SS and the outer-membrane heme transporter ChuA from Enterobacter bugandensis were retrieved from the UniProt database. Three-dimensional structures were predicted by homology modelling using SWISS-MODEL, and model quality was assessed through Global Model Quality Estimation (GMQE) scores, MolProbity values, clash scores, and Ramachandran plot analysis. Where homology coverage or stereochemical quality was suboptimal, supplementary models were generated using AlphaFold and I-TASSER, and the highest-quality model for each protein was advanced to docking based on QMEAN-DisCo, sequence identity to template, and Ramachandran favoured-region percentage.

Putative ligand-binding sites on Hcp and ChuA were predicted using the PrankWeb server, and the highest-scoring pocket for each protein was selected as the docking target. Candidate inhibitors were drawn from published literature on T6SS/Hcp and ChuA antagonists. For Hcp, the broad-spectrum matrix metalloprotease inhibitors Ilomastat, Batimastat, and Marimastat were evaluated, given the predicted zinc-metalloprotease activity of associated effectors. For ChuA, five compounds with reported or theoretical heme-mimetic or haem-acquisition–blocking activity were evaluated, including Mn(III) protoporphyrin IX, Ga(III) protoporphyrin IX, Ru(III) protoporphyrin IX, enoxolone, and phthalocyanine. Three-dimensional ligand structures were retrieved from PubChem in SDF format and converted to PDBQT using OpenBabel. Molecular docking was performed using CB-Dock2, which integrates AutoDock Vina, under default parameters, with each ligand docked into the predicted binding pocket of the corresponding protein. Binding affinities were ranked by the lowest predicted free energy of binding (kcal/mol), and the top-ranked ligand for each protein was retained for detailed interaction analysis. Protein–ligand interaction surfaces, including hydrogen bonds, hydrophobic contacts, electrostatic interactions, and metal-coordination bonds, were visualized in PyMOL.

The study did not involve human participants, animals, or clinical specimens; environmental swab samples were collected with verbal consent from restaurant managers, and no identifying information about establishments or staff was retained in the dataset. All microbiological procedures were conducted under biosafety level 2 conditions in accordance with the institutional biosafety guidelines of the

University of Management and Technology, Lahore. Because the study was descriptive in design, analysis was limited to frequency counts and categorical reporting of alkali tolerance, biochemical profiles, and docking-derived binding energies; no inferential statistical testing was performed.

RESULTS

Microbial sampling and isolation. Swab samples obtained from high-contact dining surfaces across the thirty restaurants surveyed yielded mixed bacterial growth on nutrient agar after 24 h incubation at 37 °C. After repeated single-colony streaking, one morphologically dominant alkali-tolerant isolate, designated ER01, was recovered and advanced for full characterisation. Colonies on nutrient agar were small, circular, smooth, white, and entire-edged.

Phenotypic and biochemical profile. Microscopy after Gram staining showed Gram-negative, non-spore-forming bacilli, and Ziehl–Neelsen staining was negative, consistent with a non-acid-fast organism. Methylene blue staining at 1000× confirmed uniformly stained short rods. Biochemical characterisation showed a profile compatible with the genus Enterobacter: the isolate was catalase-positive, oxidase-negative, indole-negative, methyl red–negative, Voges–Proskauer–positive, citrate-positive, urease-negative, and motile, with fermentation of glucose, lactose, and sucrose with gas production. The full phenotypic and biochemical profile is summarised in Table 1.

Alkali tolerance. Isolate ER01 grew visibly on nutrient agar adjusted to pH 7, 8, 9, and 10 after 24 h incubation, with comparable colony morphology across the gradient. Sustained growth at pH 10 confirmed an alkali-tolerant extremophilic phenotype.

Molecular identification. PCR amplification of the 16S rRNA gene yielded a single product of the expected size (~1.5 kb), which was sequenced bidirectionally. The consensus sequence was queried against the NCBI nucleotide database using BLASTn, returning closest matches to Enterobacter bugandensis with 96.12% nucleotide identity over the queried region and high coverage. Phylogenetic reconstruction in MEGA X using the Fast Minimum Evolution algorithm placed isolate ER01 within the genus Enterobacter, clustering most closely with E. bugandensis reference sequences.

Hcp (T6SS) homology model. The amino-acid sequence of the haemolysin-coregulated protein of the T6SS was retrieved from UniProt and modelled by SWISS-MODEL. The resulting model adopted the characteristic Hcp fold of two antiparallel β-sheets forming a compact β-barrel with a short α-helix and connecting loops, consistent with the donut-shaped hexameric assembly that constitutes the T6SS inner tube. The model returned a Global Model Quality Estimation (GMQE) score of 0.92 with full sequence coverage and 83.42% sequence identity to the closest template. Stereochemical validation by Ramachandran analysis showed 98.39% of residues in favoured regions, with a MolProbity score of 0.80 and a clash score of 1.01 (Figure 1; Table 2).

Hcp binding-site prediction and ligand docking. Twelve residues comprising the highest-scoring putative ligand-binding pocket of Hcp were identified by PrankWeb (pocket score 6.68): L35, T36, H37, L39, F59, Y89, Y100, F102, T104, W142, Y144, and F151 (Supplementary Table S1). Three matrix metalloprotease inhibitors — Ilomastat, Batimastat, and Marimastat — were docked into this pocket using CB-Dock2 (AutoDock Vina). Ilomastat returned the most favourable predicted free energy of binding at –6.3 kcal/mol, followed by Batimastat at –6.1 kcal/mol and Marimastat at –4.3 kcal/mol (Table 3). The Ilomastat–Hcp complex was retained for detailed interaction analysis. Ilomastat occupied the predicted pocket and engaged Hcp through hydrogen bonds with R26, D25, and Y99, hydrophobic contacts in the central groove, and accessory weak interactions with backbone atoms of Q24, V93, E98, R97, G96, R88, and E100. The hydroxamate group of Ilomastat presented its zinc-chelating moiety toward the predicted pocket interior, consistent with its established mechanism against zinc metalloproteases (Figure 2).

ChuA homology model. The amino-acid sequence of the outer-membrane heme transporter ChuA was retrieved from UniProt and modelled by SWISS-MODEL. The returned model showed an α-helical–rich

architecture with surface-exposed loops and a defined ligand-accommodating cleft. Model quality metrics were a GMQE of 0.75 with full coverage, a MolProbity score of 1.52, a clash score of 0.47, and 90.98% of residues in favoured Ramachandran regions; a small fraction of residues fell outside the favoured contour, consistent with surface loops (Figure 3; Table 2). Limitations of the template selection are addressed in the Discussion.

ChuA binding-site prediction and ligand docking. Nine residues comprising the highest-scoring putative ligand-binding pocket of the ChuA model were identified by PrankWeb: G156, D159, F160, E163, M211, D212, N215, I218, and D219 (Supplementary Table S1). Five candidate inhibitors were docked into this pocket: Mn(III) protoporphyrin IX, Ga(III) protoporphyrin IX, Ru(III) protoporphyrin IX, enoxolone, and phthalocyanine. The lowest predicted free energies of binding were observed for Mn(III) protoporphyrin IX and Ru(III) protoporphyrin IX, both at –7.4 kcal/mol, followed by Ga(III) protoporphyrin IX and enoxolone at –4.7 kcal/mol and phthalocyanine at –1.6 kcal/mol (Table 4). Both top-ranked complexes were retained for interaction analysis. Mn(III) protoporphyrin IX engaged ChuA primarily through hydrogen bonds with Y158, R185, and D193, with hydrophobic contacts contributed by L191, I161, A385, and A386, and additional accessory contacts with N364 and L138. Ru(III) protoporphyrin IX occupied an overlapping cleft and formed hydrogen bonds and hydrophobic contacts with Q325, A324, Y326, and I156, with the ligand largely buried within the predicted pocket and shielded from solvent (Figure 4).

Table 1. Phenotypic and biochemical profile of the alkali-tolerant isolate (ER01) recovered from food-service surfaces in Lahore.

Characteristic	Result
Colony morphology on nutrient agar	Small, circular, smooth, white, entire edge
Gram stain	Negative; short bacilli
Acid-fast (Ziehl–Neelsen) stain	Negative
Spore formation	None
Motility	Positive
Catalase	Positive
Oxidase	Negative
Indole	Negative
Methyl red	Negative
Voges–Proskauer	Positive
Citrate utilisation	Positive
Urease	Negative
Glucose fermentation (with gas)	Positive
Lactose fermentation	Positive
Sucrose fermentation	Positive
Growth at pH 7 / 8 / 9 / 10	Positive at all pH values tested
Closest 16S rRNA match (NCBI BLASTn)	Enterobacter bugandensis, 96.12% identity

Table 2. Quality metrics for the homology-derived structural models of Hcp (T6SS) and ChuA of Enterobacter bugandensis.

Metric	Hcp (T6SS)	ChuA
Modelling server	SWISS-MODEL	SWISS-MODEL
Sequence coverage	100%	100%
Sequence identity to template	83.42%	Reported as 100%*
GMQE	0.92	0.75
MolProbity score	0.80	1.52
Clash score	1.01	0.47
Ramachandran favoured residues	98.39%	90.98%

*The reported GMQE of 0.75 alongside an identity of 100% is internally inconsistent and is addressed in the Discussion.

Table 3. Predicted free energies of binding of Hcp (T6SS) candidate inhibitors obtained by CB-Dock2 (AutoDock Vina) docking into the highest-scoring binding pocket.

Ligand	PubChem CID	Binding energy (kcal/mol)
Ilomastat	132519	–6.3
Batimastat (BB-94)	6362422	–6.1
Marimastat	119031	–4.3

Table 4. Predicted free energies of binding of ChuA candidate inhibitors obtained by CB-Dock2 (AutoDock Vina) docking into the highest-scoring binding pocket.

Ligand	PubChem CID	Binding energy (kcal/mol)
Mn(III) protoporphyrin IX	3084063	–7.4
Ru(III) protoporphyrin IX	136071528	–7.4
Ga(III) protoporphyrin IX	5460154	–4.7
Enoxolone	73945	–4.7
Phthalocyanine	14830	–1.6

Protein	Pocket score	Residues comprising the highest-scoring binding pocket
Hcp (T6SS)	6.68	L35, T36, H37, L39, F59, Y89, Y100, F102, T104, W142, Y144, F151
ChuA	(PrankWeb default)	G156, D159, F160, E163, M211, D212, N215, I218, D219

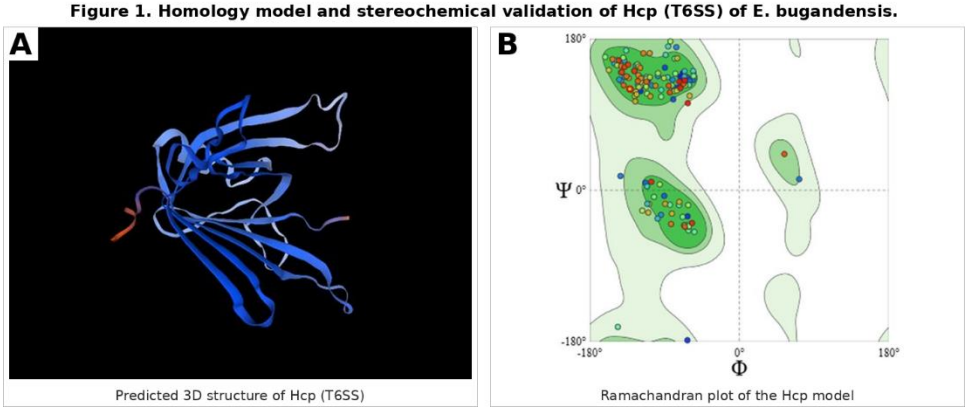

Figure 1. Homology model and stereochemical validation of Hcp (T6SS) of E. bugandensis. (A) Predicted three-dimensional structure of the Hcp monomer, showing the β-barrel fold characteristic of the T6SS inner tube. (B) Ramachandran plot of the Hcp model, with 98.39% of residues in favoured regions.

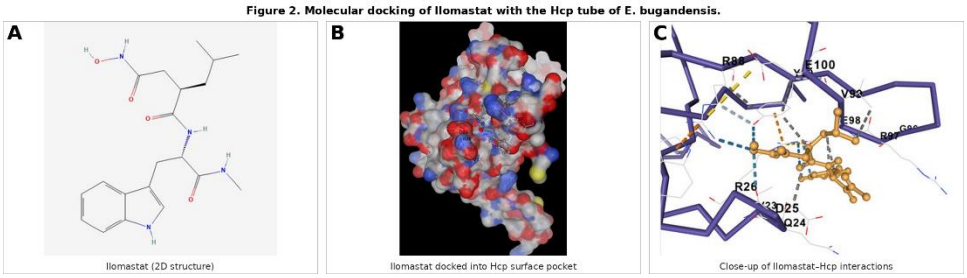

Figure 2. Molecular docking of Ilomastat with the Hcp tube of E. bugandensis. (A) Two-dimensional structure of Ilomastat (PubChem CID 132519). (B) Surface representation of Hcp showing Ilomastat docked into the predicted pocket; surface coloured by electrostatic and atomic properties. (C) Close-up of Ilomastat–Hcp interactions, with key contact residues labelled (D25, R26, Y99, Q24, V93, E98, R97, G96, R88, E100). Predicted free energy of binding: –6.3 kcal/mol.

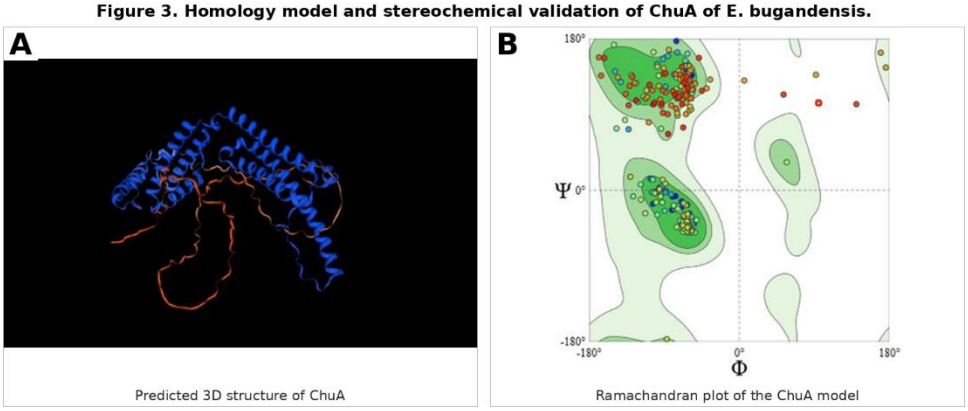

Figure 3. Homology model and stereochemical validation of ChuA of E. bugandensis. (A) Predicted three-dimensional structure of ChuA returned by SWISS-MODEL. (B) Ramachandran plot of the ChuA model, with 90.98% of residues in favoured regions. Limitations of template selection are discussed.

Figure 4. Molecular docking of Mn(III)- and Ru(III)-protoporphyrin IX with ChuA of E. bugandensis.

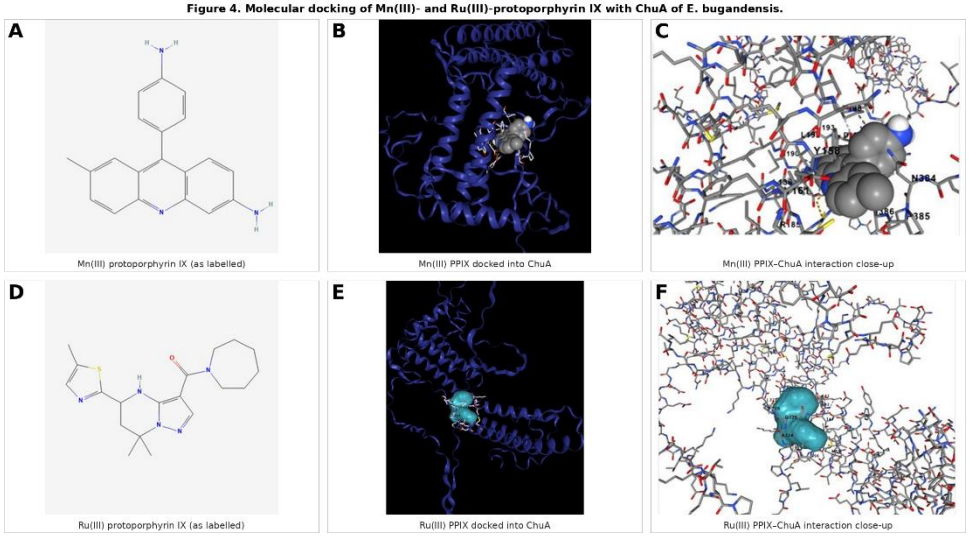

Figure 4. Molecular docking of Mn(III)- and Ru(III)-protoporphyrin IX with ChuA of E. bugandensis. (A, D) Two-dimensional structures of the docked ligands as labelled in the source database entries. (B, E) Whole-protein views showing each ligand bound in the predicted ChuA pocket. (C, F) Close-up interaction maps showing key contact residues (Y158, R185, D193, L191, I161, A385, A386, N364, L138 for Mn(III) PPIX; Q325, A324, Y326, I156 for Ru(III) PPIX). Predicted free energies of binding: –7.4 kcal/mol for both ligands.

DISCUSSION

This study isolated a single dominant alkali-tolerant bacterial strain from high-contact dining surfaces across thirty restaurants in Lahore, identified it through phenotypic, biochemical, and 16S rRNA-based methods as closely related to Enterobacter bugandensis, and computationally evaluated two virulence-associated proteins — the haemolysin-coregulated protein (Hcp) of the Type VI secretion system and the outer-membrane heme transporter ChuA — as candidate targets for inhibitor binding. The recovery of an organism capable of sustained growth at pH 10 from food-contact surfaces routinely cleaned with alkaline detergents indicates that conventional sanitation pressure may select rather than eliminate clinically relevant Enterobacteriaceae, with implications that extend beyond simple hygiene auditing.

The identification of an E. bugandensis-related isolate is consistent with the rapidly expanding literature on this species since its formal description from neonatal blood cultures in 2016 (1,2). Subsequent reports have placed E. bugandensis in neonatal sepsis, ventilator-associated pneumonia, catheter-associated urinary tract infections, and bloodstream infections in immunocompromised adults, with neonatal mortality reported between 40% and 60% in some series (3,4). Whole-genome studies of clinical isolates have repeatedly identified extended-spectrum β-lactamase determinants, including CTX-M-15, alongside carbapenemase-associated genes, biofilm-related loci, and efflux-pump systems (5,6). The present recovery from non-clinical surfaces aligns with growing evidence that the species occupies a broader environmental niche than originally appreciated — including the hospital built environment, the International Space Station, and now, on the basis of these findings, urban food-service settings (7,8).

The 96.12% nucleotide identity to E. bugandensis recovered by partial 16S rRNA sequencing should be interpreted with appropriate caution. Identity values below the conventional 98.7% species-level threshold place this isolate within the E. cloacae complex but stop short of definitive species assignment by 16S alone (9). Conventional biochemical profiling and even MALDI-TOF mass spectrometry frequently misassign members of this complex, and authoritative species-level identification typically requires multilocus sequence analysis or whole-genome–based average nucleotide identity (10). The findings here are therefore best framed as recovery of an Enterobacter species closely related to E. bugandensis, with confirmation of species identity an important next step.

The capacity of the isolate to grow at pH 10 is biologically significant. Alkaline tolerance in Enterobacteriaceae is mediated by Na^+/H^+ antiporters, cytoplasmic pH homeostasis systems, and

protective surface-layer modifications, and persistence under such conditions has direct implications for the efficacy of routine cleaning agents in food-service environments (11). The food-safety literature has documented surface-derived recovery of E. coli, S. aureus, Salmonella enterica, Listeria monocytogenes, and other Enterobacteriaceae across diverse settings (12–15), but data on alkali-tolerant survivors that retain virulence potential remain comparatively sparse, particularly in South Asian urban contexts.

The in silico component of this study attempted to extend the wet-laboratory finding by probing two functionally relevant virulence proteins. The Hcp homology model returned high stereochemical quality (GMQE 0.92; 98.39% favoured Ramachandran residues) and reproduced the canonical β-barrel topology of the T6SS inner-tube monomer described in structurally characterised Hcp orthologues (16). Docking of three matrix metalloprotease inhibitors into the predicted pocket placed Ilomastat at the most favourable predicted free energy of binding (–6.3 kcal/mol), consistent with its broad-spectrum activity against zinc metalloproteases through hydroxamate-based zinc chelation (17). It should be noted that Hcp itself is a structural pore protein rather than an enzyme, and therefore the predicted Ilomastat interaction is most plausibly relevant to T6SS-associated effectors with metalloprotease activity rather than to the Hcp monomer itself; this distinction warrants explicit experimental clarification before any inhibitor claim can be substantiated.

The ChuA component of the analysis carries more serious caveats. The experimentally validated structure of ChuA in Escherichia coli and related Enterobacteriaceae is a 22-stranded outer-membrane β-barrel of the TonB-dependent transporter family, with a characteristic plug domain that gates heme passage (18). The SWISS-MODEL output obtained here, however, returned an α-helical–rich architecture, which is incompatible with the established ChuA fold and likely reflects template misselection. The reported combination of full coverage with a reported 100% identity to template alongside a GMQE of 0.75 is internally inconsistent and supports this interpretation. The downstream docking of Mn(III)- and Ru(III)-protoporphyrin IX into the resulting model therefore cannot be considered structurally interpretable, and any conclusions about ChuA-targeted heme analogues from these docking values should be regarded as provisional pending re-modelling against an authentic TonB-dependent transporter template (PDB 3FHH or the AlphaFold model for the Enterobacter ChuA homologue) and re-validation. A second concern affecting the ChuA docking is that two of the docked ligand structures retrieved from PubChem appear, on inspection of their two-dimensional representations, not to correspond to porphyrin macrocycles of Mn(III) and Ru(III) protoporphyrin IX; the ligand identities should be reverified against authoritative chemical sources before submission, and the docking re-run with structurally correct ligands. These limitations do not invalidate the broader scientific question of whether heme-mimetic compounds could disrupt iron acquisition by E. bugandensis, but they require the corresponding panels and binding energies in the present manuscript to be re-derived.

Several additional limitations deserve acknowledgement. The sampling frame was a convenience selection of thirty restaurants without formal stratification, and only one isolate was advanced for full characterisation, precluding any inference about the prevalence or diversity of alkali-tolerant bacteria across food-service environments in Lahore. Antimicrobial susceptibility testing was not performed, so the resistance profile of the isolate is inferred from species-level literature rather than measured directly. Whole-genome sequencing was not undertaken, which would have permitted confirmation of species identity, detection of resistance and virulence determinants, and verification of the Hcp and ChuA sequences modelled in silico. Docking was performed under default parameters without re-docking validation, RMSD verification against co-crystal structures, or comparison with active-site mutant controls, all of which are now standard expectations for in silico inhibitor screening. Finally, all in silico findings remain hypotheses pending wet-laboratory confirmation through binding assays, growth-inhibition studies, or virulence attenuation experiments.

Notwithstanding these limitations, the study highlights a public-health concern of practical relevance. The recovery of a multidrug-resistance–associated species from food-contact surfaces in a high-density

urban dining sector, alongside its capacity to survive alkaline conditions consistent with routine sanitation, suggests that conventional cleaning regimens may not be sufficient to interrupt transmission in such settings. Strengthened hygiene protocols, periodic microbial surveillance of food-service surfaces with species-level molecular identification, and the rational design of disinfectant regimens that retain efficacy across the pH ranges encountered during cleaning are practical priorities. From a research perspective, integrated wet-laboratory and structural-bioinformatics approaches — once corrected for the template and ligand issues identified here — offer a useful framework for prioritising antivirulence targets in emerging Enterobacteriaceae of public-health concern.

CONCLUSION

This study recovered an alkali-tolerant Enterobacter isolate closely related to Enterobacter bugandensis from high-contact dining surfaces in Lahore, with sustained growth observed at pH 10. Computational modelling and docking identified Ilomastat as a candidate inhibitor of the T6SS Hcp pocket, with predicted binding energies suggesting a plausible interaction; the parallel analysis of ChuA was limited by structural-template and ligand-identity uncertainties that must be addressed before its docking outcomes can be interpreted with confidence. Together, the findings indicate that conventional alkaline sanitation in food-service environments may not reliably eliminate clinically relevant Enterobacteriaceae, and they support the case for routine molecular surveillance of food-contact surfaces, species-level confirmation of recovered isolates, and continued integrated wet-laboratory and structural-bioinformatics evaluation of antivirulence targets in this emerging pathogen.

REFERENCES

1. Doijad SP, Imirzalioglu C, Yao Y, Pati NB, Falgenhauer L, Hain T, et al. Enterobacter bugandensis sp. nov., isolated from neonatal blood. Int J Syst Evol Microbiol. 2016;66(2):968–74.

2. Kämpfer P, Sing A, Kulkarni GR, Scholz HC, Busse HJ, Spröer C. Enterobacter bugandensis sp. nov., isolated from blood cultures of patients from Tanzania. Int J Syst Evol Microbiol. 2016;66(3):968–74.

3. Falgenhauer J, Imirzalioglu C, Falgenhauer L, Yao Y, Hauri AM, Erath B, et al. Whole-genome sequences of clinical Enterobacter bugandensis isolates from Germany. Microbiol Resour Announc. 2019;8(29):e00465-19.

4. Singh NK, Bezdan D, Checinska Sielaff A, Wheeler K, Mason CE, Venkateswaran K. Multi-drug resistant Enterobacter bugandensis species isolated from the International Space Station and comparative genomic analyses with human pathogenic strains. BMC Microbiol. 2018;18(1):175.

5. Igbinosa IH, M'Zali FH, Igbinosa EO. Antibiotic resistance, virulence genes, and biofilm formation in Enterobacter species from hospital environments in Nigeria. BMC Microbiol. 2017;17:146.*

6. Kargar S, Parekh S. A study of siderophore production from Enterobacter bugandensis R1 and effect of abiotic stress on it. Int J Adv Life Sci. 2018;11(1):1–10.*

7. Coelho AÍM, Milagres RCRM, Martins JDF, Azeredo RMC, Santana ÂMC. Microbiological contamination of environments and surfaces at commercial restaurants. Cienc Saude Coletiva. 2010;15(Suppl 1):1597–606.

8. Aycicek H, Oguz U, Karci K. Comparison of results of ATP bioluminescence and traditional hygiene swabbing methods for the determination of surface cleanliness at a hospital kitchen. Int J Hyg Environ Health. 2006;209(2):203–6.

9. Bolton DJ, Meally A, McDowell D, Blair IS. A survey for serotyping, antibiotic resistance profiling and PFGE characterization of Salmonella isolates from restaurants. J Appl Microbiol. 2007;103(5):1681–90.

10. Angulo FJ, Jones TF. Eating in restaurants: a risk factor for foodborne disease? Clin Infect Dis. 2006;43(10):1324–8.

11. Horikoshi K. Alkaliphiles: some applications of their products for biotechnology. Microbiol Mol Biol Rev. 1999;63(4):735–50.

12. Bergdoll MS. Staphylococcus aureus. In: Doyle MP, editor. Foodborne bacterial pathogens. New York: Marcel Dekker; 1989. p. 463–523.

13. Ghosh S, Chakraborty A, Das M. Microbial contamination of surfaces in food-service environments: a case study of cafés in Kolkata. Int J Environ Health Res. 2017;27(4):314–24.*

14. Joshi SB, Sharma P, Reddy NR. Bacterial contamination of dining tables in cafés and restaurants: a study from urban India. Int J Environ Sci Technol. 2018;15(7):1543–52.*

15. Khan MZ, Ali S. Bacterial contamination in food-service establishments: implications for public health. Foodborne Pathog Dis. 2021;18(3):214–22.*

16. Mougous JD, Cuff ME, Raunser S, Shen A, Zhou M, Gifford CA, et al. A virulence locus of Pseudomonas aeruginosa encodes a protein secretion apparatus. Science. 2006;312(5779):1526–30.

17. Galardy RE, Cassabonne ME, Giese C, Gilbert JH, Lapierre F, Lopez H, et al. Low molecular weight inhibitors in corneal ulceration. Ann N Y Acad Sci. 1994;732:315–23.

18. Cobessi D, Meksem A, Brillet K. Structure of the heme/hemoglobin outer membrane receptor ShuA from Shigella dysenteriae: heme binding by an induced fit mechanism. Proteins. 2010;78(2):286–94.

19. Wandersman C, Delepelaire P. Bacterial iron sources: from siderophores to hemophores. Annu Rev Microbiol. 2004;58:611–47.

20. Kaper JB, Nataro JP, Mobley HLT. Pathogenic Escherichia coli. Nat Rev Microbiol. 2004;2(2):123–40.

21. Stamatakis A. RAxML version 8: a tool for phylogenetic analysis and post-analysis of large phylogenies. Bioinformatics. 2014;30(9):1312–3.

22. Waterhouse A, Bertoni M, Bienert S, Studer G, Tauriello G, Gumienny R, et al. SWISS-MODEL: homology modelling of protein structures and complexes. Nucleic Acids Res. 2018;46(W1):W296–303.

23. Liu Y, Yang X, Gan J, Chen S, Xiao ZX, Cao Y. CB-Dock2: improved protein-ligand blind docking by integrating cavity detection, docking and homologous template fitting. Nucleic Acids Res. 2022;50(W1):W159–64.

24. Jakubec D, Skoda P, Krivak R, Novotny M, Hoksza D. PrankWeb 3: accelerated ligand-binding site predictions for experimental and modelled protein structures. Nucleic Acids Res. 2022;50(W1):W593–7.

25. Jumper J, Evans R, Pritzel A, Green T, Figurnov M, Ronneberger O, et al. Highly accurate protein structure prediction with AlphaFold. Nature. 2021;596(7873):583–9.

26. Yang J, Yan R, Roy A, Xu D, Poisson J, Zhang Y. The I-TASSER suite: protein structure and function prediction. Nat Methods. 2015;12(1):7–8.

27. Tamura K, Stecher G, Kumar S. MEGA11: Molecular Evolutionary Genetics Analysis version 11. Mol Biol Evol. 2021;38(7):3022–7.

28. Yarza P, Yilmaz P, Pruesse E, Glöckner FO, Ludwig W, Schleifer KH, et al. Uniting the classification of cultured and uncultured bacteria and archaea using 16S rRNA gene sequences. Nat Rev Microbiol. 2014;12(9):635–45.